MECHANICAL PROPERTIES OF FIBRE-REINFORCED COMPOSITES TESTED UNDER SUPERPOSED HYDROSTATIC PRESSURES

ROYAL ARMAMENT RESEARCH AND
DEVELOPMENT ESTABLISHMENT

NOVEMBER 1975

20000726024

$\textcircled{2}$

MINISTRY OF DEFENCE

ROYAL ARMAMENT RESEARCH AND DEVELOPMENT ESTABLISHMENT

RARDE TECHNICAL REPORT 10/75

DA024376

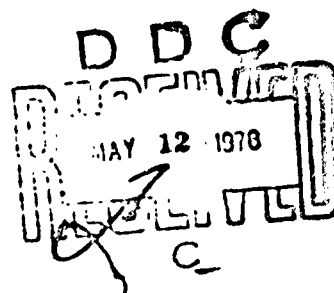### Mechanical properties of fibre-reinforced composites tested under superposed hydrostatic pressures

B R Watson-Adams
J J Dee
A S Wronski

Fort Halstead
Kent

November
1975

Mechanical properties of fibre-reinforced composites
tested under superposed hydrostatic pressures

B R Watson-Adams, M Sc, LIM
J J Dibb, B Tech (University of Bradford)
A S Wronski, Ph D (University of Bradford)
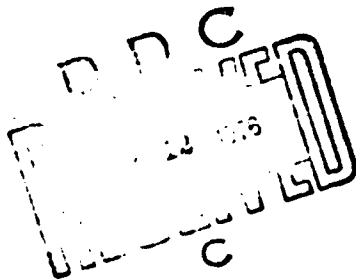
Summary

See page 2.

Summary

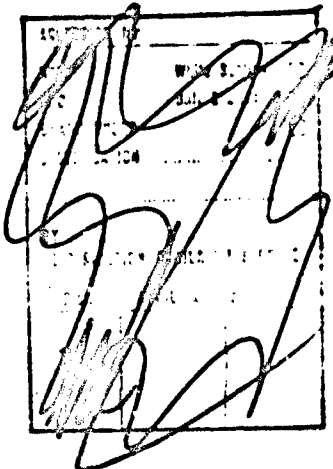In glass or carbon fibre/resin composites theoretical tensile strengths are rarely realised; good composites produced by reproducible conventional techniques attain about 60% of the theoretically predicted values, σ_{th}. In an attempt to improve the tensile properties 54% V_f carbon and 60% V_f glass fibre/epoxy resin rods were manufactured by pultrusion and values of ~80% σ_{th} were obtained. Although the fibres are continuous, these properties suggest that perhaps an "effective discontinuous fibre length" is an important composite parameter. It is thus possible to account for the "random bundle break" appearance of fracture surfaces. Either frictional properties of the fibre/resin interface or the shear failure stress of the resin would then play an important role in determining tensile strength; results of tests on resin and carbon fibre composite specimens under superposed hydrostatic pressures between 100 and 280 MNm^{-2} indicate the critical property to be the resin shear failure stress. It is suggested that the proposed hypotheses, of direct relevance to the design of composite systems and design with fibre-reinforced materials, should be tested by further experiments. Of particular importance is the increase to 90% σ_{th} of the composite strength when tested under a superposed pressure of 40 MNm^{-2}.

53% V_f carbon fibre/nickel composites were prepared by the RARDE technique of plating and hot compaction. The reproducible tensile strength, nearly 60% σ_{th}, was superior to values reported by other laboratories; however, only a marginal improvement in toughness was observed. In tension, nevertheless, the nickel matrix was ductile, in contrast to the material of Braddick et al. Tests under superposed hydrostatic pressures indicate the critical stage in the failure process to be the tensile failure of the fibres, in contrast to the shear-operated failure mechanism in the resin composite.

CONTENTS

In the study of the mechanical properties of fibre-reinforced materials increasing emphasis is now being paid to the role of the fibre/matrix interface in the mechanisms of fracture. In the simplest failure model (1) it is assumed that an equal strain exists in the fibres and the matrix and that fracture occurs when the failure strain of the fibres is reached. Outwater (2) has postulated that for some resin matrix composites debonding will occur with a shear line starting at the ends of the fibres and moving to the middle. Stresses, he suggests, are transferred from the matrix to the fibres by friction rather than shear. Failure may occur by either complete debonding, or if the bond is sufficiently good, by matrix shear or failure of the fibres.

The effect of fibre flaws linked with non-uniform strain distribution has been studied by Parratt (3) who suggests that as the load on a specimen increases, the number of internal fibre fractures increases, shortening the fibre lengths to the point where the ultimate shear strength of the matrix is exceeded and composite failure takes place through shear failure of the matrix. The statistical model of Rosen (4,5), supported by results from a photo-elastic study of the tensile failure process, again indicates that fibre fractures occur randomly, starting at about half the composite strength On this model the strength of the composite is determined by the statistical strength characteristics of the fibres and by the efficiency with which the matrix is able to redistribute the high shear stresses which exist in the vicinity of a fibre break. A composite with a ductile matrix would thus be expected to be stronger than one with a brittle matrix.

It is generally recognised that the bundle strength, σ_B, of an assembly of parallel fibres is always less than the mean strength of the fibres (measured at the same length). For a typical scatter of $\pm$ 20% of the average (6) the fibre bundle can only achieve ~ 70% of the mean fibre strength. Measurement of bundle strength has been suggested (6) as a useful method of incorporating statistical factors into composite strength predictions of fibre/resin composites by the relationship;

$$\sigma_c = V_f \, \sigma_B \; (L) \approx 0.7 \; V_f \; \sigma_f$$

where σ_c is the composite strength, V_f the volume fraction of the fibres of mean breaking strength σ_f and the gauge length of the fibre bundle (L) is the same as the composite specimen gauge length. This uncoupled statistical model represents the lower estimate of the theoretical composite strength (6).

The theory of the load carrying capacity of uniaxially loaded composites has been developed in some detail (7-9). In general, for continuous fibres the strength of a composite is given by:

$$\sigma_c = \sigma_f \, V_f + \sigma'_m \; (1-V_f)$$

where σ'_m is the stress in the matrix at the fracture strain of the fibres.

For discontinuous fibres of length L, strengthening is always less. The tensile and shear stress distributions are given in Fig 1. The tensile stress in the fibre builds up rapidly from each end approximately linearly, ie:-

$$\sigma_z = \frac{2\tau z}{r}$$

where τ is the maximum matrix or interface shear stress, r the fibre radius and z is the distance from the end of the fibre, smaller than $\frac{1}{2}L$ and the critical value $\frac{1}{2}L_c$, to be defined.

At the fracture stress σ_f of the fibre $z = \frac{r \sigma_f}{2\tau}$ and hence before it can be broken the fibre must be of a critical length $L_c = 2z$.

If d is the diameter, then:-

$$L_c = \left(\frac{\sigma_f \, d}{2\tau}\right)$$

When the fibre length is less than L_c the fracture stress of the fibre is never reached. When $L = L_c$ the fibre will break in the centre and the average stress σ'_f over the fibre is $\frac{\sigma_f}{2}$. When $L > L_c$, $\bar{\sigma}_f$ approaches σ_f and the strength of the composite is given by:-

$$\sigma_c = \bar{\sigma}_f V_f + \sigma'_m \left(1-V_f\right) = \sigma_f V_f \left(1 - \frac{L_c}{2L}\right) + \sigma'_m \left(1-V_f\right)$$

The aim of the work described here is the investigation of the mechanisms of the failure of fibre composites and the study of the importance of the fibre, matrix, and fibre/matrix interface in the strengthening of such a composite. Unidirectional glass and carbon fibre reinforced epoxy resin specimens produced by a pultrusion technique were used in the study of resin matrix composites, and carbon fibre reinforced nickel fabricated by a plating and hot compaction technique was used for the study of the metal matrix composite.

The experimental technique involved the use of hydrostatic pressure during tensile tests. Under ambient conditions, for an applied tensile stress σ, the maximum shear stress is given as $\frac{\sigma}{2}$ (Fig 2). Under a hydrostatic pressure H and an applied tensile stress σ the nett tensile stress is $\sigma-H$, but the maximum shear stress is still $\frac{\sigma}{2}$. At the same nett tensile stress, σ, therefore, the maximum shear stress is $\frac{\sigma + H}{2}$. Using hydrostatic pressure the tensile to shear stress ratio may thus be varied. As the transfer of load from the matrix to the fibres involves shear stresses in the matrix and at the interface, then variable hydrostatic pressure techniques are important in determining the mechanism of failure. The application of hydrostatic pressure has previously been used in the study of mechanical properties of metals, ceramics and thermoplastics.

Composite fabrication: resin matrix composites (10)

One of the undesirable characteristics of mechanical tests on fibre-reinforced plastic (FRP) specimens has frequently been the large scatter in results. This has principally been ascribed to the presence of voids and misalignment in the fibres, lack of adhesion between fibres and matrix, defects in the fibres themselves and differences in the gauge length of specimens tested. As the first three factors depend on the fabrication process, pultrusion appears to offer a possible means of improvement on the wet lay-up method. Pultrusion, the technique of pulling continuous lengths of resin-soaked fibre through a heated die, has been developed for glass fibres and recently applied to carbon fibres by Garnett et al (11). A modified form of their apparatus was used in the Process Technology Division, AERE, Harwell, to manufacture the resin matrix composites used in our investigation. The pultrusion rig, Fig 3, consisted of four sets of tensioning rollers/fibre guides, 2 PTFE sizing dies for removing air bubbles, improving fibre impregnation and removing excess resin and a third curing die 75mm long and 6.35mm in diameter, which was thermostatically heated. The entrance to the die was cooled by a water jacket to prevent premature gelling of resin which tended to build up at the throat. For the system Araldite MY753/HT951 resin/54% carbon fibres and 60% glass fibres the optimum conditions based on carbon fibre/resin exotherms were found to be a die exit temperature of $140^{\circ}C$ and a pulling speed of 20mm/min. The carbon fibres were Harwell Type II surface treated with a mean strength of 2240 KNm^{-2} and a mean diameter of 9.08 μm. The glass fibres were Owens Corning Type 810EC. The fibres were pulled by means of a steel cord cast, via a brass screw, into the end of the 4 fibre bundles. The rods produced were 1.2m long and were post-cured for 1 hour at $100^{\circ}C$.

Composite fabrication: nickel matrix composite (12)

(plating and compaction)

One of the more useful techniques for producing carbon fibre-reinforced metal composites is electroplating of the fibres, followed by hot compaction. Recently Kistler and Niess (13), Braddick, Jackson and Walker (14) and Donovan and Watson-Adams (15) have reported on the production of carbon fibre-nickel composites by this method. A modification of the last technique was used to produce the composite for this investigation.

The plating rig, Fig 4, consisted of a cylindrical cage with fibre tows vertically aligned on it, which was slowly rotated in a thermostatically controlled Watts Type Bath (Table 1) at $37^{\circ}C$. A low current density of 1.6 Am^{-2} was applied for 24 hours to obtain an even nickel coating (Fig 5). The plated fibres were thoroughly washed in running water at $50^{\circ}C$, followed by distilled water, then allowed to dry. The thickness of the plating was ~1.8 μm.

The hot compaction was carried out in a Nimonic mould (Fig 6) between carbon blocks which provide a reducing atmosphere. 1.5×10^{6} plated fibres 100mm

in length were aligned between nickel foils in the mould and a small
retaining pressure was applied. Pressure and temperature were then
increased over a period of 40 minutes to 95 KN m^{-2} and 700°C. These
conditions were maintained for 2 hours, after which the mould was allowed
to cool, still under pressure. Rectangular bars 100mm x 25mm x 6mm were
thus produced. The fibre volume fraction, found by dissolution of the
nickel matrix and accurate weighing, was 53%.

Optical micrographs were taken of sections of the as-plated fibres (Fig 5)
and the nickel and resin matrix composites (Figs 7 and 8) and similarly
the of longitudinal sections (Figs 9 and 10).

Testing of composites

The round tensile specimen design (Fig 11) used in the present investigation
had to be developed (10) as there is no definite standard at present. Flat
specimens are generally used with fibre-reinforced resin composites and
round specimens, similar to our design, are often used for fibre-reinforced
metals.

A requirement was the design of a miniature specimen that would fit in the
very limited space of the high pressure testing apparatus. In general,
where composite modulus is not required, waisted specimens with no parallel
gauge section are accepted. The length of the shoulder was calculated from
the interlaminar shear strength of the composite, so as to prevent the
shoulder pulling off. The design had so far proved completely successful.

Tensile tests were carried out at an extension rate of 5×10^{-4} mm/min
under superposed hydrostatic pressures in the range atmospheric pressure to
280 KNm^{-8} in a Universal Hedeby testing machine (Fig 12). The effects of
hydrostatic pressure were also determined on pure resin and pure nickel
specimens (the latter having been previously annealed at 700°C for 2 hours
in the compaction rig). Scanning electron micrographs were taken of the
fracture surfaces of specimens broken at atmospheric and under hydrostatic
pressures (Figs 14 and 15).

High temperature treatments

It has been suggested that the results of tests on plated single fibres are
applicable to bulk composites. To assess the high temperature capabilities
of the bulk composite plated fibres were accordingly used. The strength of
as-plated fibres was determined as the mean of 27 tests using a gauge length
of 50mm. A tow of plated fibres was then treated under a vacuum of $\sim 10^{-6}$
torr for 24 hours at 1050°C and a similar number of tests carried out on the
heat treated fibres. Plated fibres were also treated under the same
conditions in a sealed, pre-evacuated tube containing a small quantity of
pure carbon powder.

Impact tests

A few Charpy impact tests were carried out for comparison of the fracture
toughness of the carbon fibre/nickel composite with that of other workers
(14). As the toughness of metal matrix composites frequently decreases with

increasing V_f(16), carbon fibre/nickel composite blocks were prepared with V_f in the range 20% to 70% for this investigation.

3. RESULTS

Fibre tests

The strengths of unplated and plated fibres before and after various high temperature treatments are shown in Table 2. Taking into account the strength of the nickel coating, the strength of coated fibres is somewhat higher than that of the unplated fibres, as also seems to be the strength of the fibres treated with carbon in the sealed envelope. It is to be noted that the mean diameter of the fibres in the last case was 9.00 μm as compared with 9.08 μm of the unplated fibres and 12.6 μm of the plated fibres. Treatment of the plated fibres in vacuo causes a large drop in strength. The difficulties of mounting and testing such weak and brittle fibres prevented more than three successful tests being carried out.

Matrix materials tests

Using the composite test specimen design, nickel was strained at atmospheric and superposed hydrostatic pressures. Atmospheric tests showed that this design underestimated the yield stress but resulted in values for the ultimate tensile strength similar to those obtained with specimens possessing a reduced gauge length. The yield strength of the nickel (0.27 GNm^{-2}) was unaltered by the application of hydrostatic pressure.

Specimens machined from cast epoxy rods were similarly tested and the pronounced effect of hydrostatic pressure on the tensile strength was noted (Fig 13). The tensile strength σ_T decreased approximately linearly with the superposed hydrostatic pressure but the shear strength, $\dfrac{\sigma_T + H}{2}$, (equal to

half the nominal ultimate applied stress σ_A) increased from 32 MNm^{-2} with pressure with a slope of 0.11.

The appearance of the failure surfaces of the tensile specimen changed from the normal polymer failure mode (Fig 14) originating at the surface to a lip of shear failure and a featureless "mirror" central fracture at 300 MNm^{-2} (Fig 15). The final break could have been caused by the fluid penetrating into the failing specimen.

Composites

The mean tensile strength of the carbon fibre reinforced epoxy resin composite was 0.93 ± 0.05 GNm^{-2} and that of the carbon fibre reinforced nickel composite was 0.73 ± 0.05 GNm^{-2}. The effect of superposed hydrostatic pressure can be seen in Fig 16. Note that the applied tensile stress σ_A, not $\sigma_A - H$, is plotted. In the case of the nickel matrix composite, the applied stress increases with increasing hydrostatic pressure with the slope ~1.0, ie the strength is unaffected by hydrostatic pressure. The behaviour

of the epoxy resin matrix composite is complex and reference to Fig 17b shows the principal axial stress σ_A-H at the point of failure for the composite and for the matrix material. It is seen that the strength of the composite first increases with hydrostatic pressure up to about 40 KPa, approximately linearly, then decreases to well below the atmospheric pressure value. Note that the composite strength increases with pressure only under stress conditions such that the tensile stress in the resin (determined when tested alone) is its maximum principal stress.

The appearance of the fracture surfaces of the resin matrix composite changes considerably with applied hydrostatic pressure (Figs 18 and 19); the amount of fibre pull-out decreasing with increasing pressure as the mode appeared to change from "random bundle" to "statistical accumulation" type of fracture. For the metal matrix composite (Fig 20) the nickel failure mode changes with increasing hydrostatic pressure, at ~ 140 KPa, from transgranular shear to intergranular rupture, the result of increasing the shear stresses in the matrix to beyond the grain boundary strength.

Impact tests

Tests on miniature Charpy specimens were carried out on the 53% V_f carbon fibre nickel composite in the temperature range 20-500°C and the value of the fracture energy was apparently independent of temperature $(1.9 \pm 0.3) 10^{-4}$ J^{-2}, ie only slightly higher than the values of Braddick et al (14) and 15% of the value for pure nickel. It is interesting to note, however, that the failure of the nickel was again entirely ductile, Fig 21. The effect of varying V_f on toughness is presented in Table 3.

4. DISCUSSION

The results of the heat treatment of plated fibres show large drops in the failure strength. Jackson and Marjoram (17) found similar results on microcomposites, but in contrast Barclay and Bonfield (18), who tested individual Type I carbon fibres coated with evaporated nickel and annealed in a vacuum of < 10 torr, found much smaller reductions in strength.

For our plated fibres annealing in a vacuum of ~ 10^{-6} torr produced a loss of strength from 1.56 $\pm$ 0.25 to 0.092 $\pm$ 0.004 GPa, but heat treatment in a closed tube with pure carbon powder resulted in the loss of almost all the nickel from the fibres, whose strength was not diminished, being 2.41 $\pm$ 0.55 compared with 2.24 $\pm$ 0.39 GPa of the unplated fibres. The problem of heat treatment of carbon fibre/nickel composites is continuously and extensively discussed and no clear explanation of the phenomenon emerges. Our results are thus presented without comment solely to make the data more extensive.

When considering the strengthening mechanisms in composites, where the fibre/matrix bond is good and the matrix is able to redistribute the high shear stresses produced at the fibre/matrix interface near a fibre break, the predicted effect of increasing hydrostatic pressure on the fracture behaviour is to increase the applied tensile stress at failure by an amount equal to the hydrostatic pressure, ie the theoretical slope would be 1

provided the flow properties of the matrix are unaffected. The results
for carbon fibre/nickel show a slope of ~ 1.0, which indicates that fracture
in this composite probably results from the tensile failure of the fibres
before either debonding or matrix failure takes place. The nett effect of
applied hydrostatic pressure on the tensile strength of the composite is
thus approximately zero. At the same time, however, the maximum shear stress
has risen, resulting in the change in matrix fracture mode from the shear to
the intergranular rupture (Fig 20). The strength of the composite, although
well reproducible, is only ~ 60% of the theoretical value. This compares
favourably with ~ 5C% reported by Braddick et al (14) but falls short of the
65% occasionally obtained by Kistler and Niesz (13). They attributed the
strength increase to a reduced amount of fibre damage and improved alignment
gained by the use of radial compaction (as opposed to unidirectional
compaction used by Braddick et al and ourselves).

In the case of the resin matrix composites a different mechanism is
indicated. There the composite strength is strongly linked with matrix
behaviour, as examination of Fig 17 makes evident.

If there were no change in the shear failure strength of the matrix with
pressure and it controlled the failure process, there would be a linear
decrease of composite strength with pressure, ie a slope of -1 on Fig 17(b)
and a slope of 0 on Fig 17(a) would result. The resin shear strength
however, increases with pressure with a slope of ~ 0.1 (Fig 13); Bowden (19)
similarly has reported a slope of about 0.2 for another resin. He also
noted an equivalent increase in the bond strength between fibre and matrix
with increasing pressure up to about 50 MNm^{-2}.

In general, the law of mixtures is used to calculate the strength of a
composite. This neglects Poisson's ratio ν (20), although the effect of
this has been calculated, it is normally negligible, particularly for
metal matrix composites, as it depends on the difference between the values
for the fibres, ν_f, and the matrix, ν_m, (21). Kelly has shown that

$$\sigma_C = E_1 V_1 e + E_2 V_2 e + 2 (\nu_2 - \nu_1) p V_1$$

where e is the strain, subscripts 1 and 2 refer to the components in smaller
and greater concentration respectively, E is Young's modulus and p is the
pressure at the interface. If we neglect effects due to the composite per
se, equate therefore p with H, and consider substance 1 to be the resin
matrix ($\nu \approx 0.4$) and 2 to be the carbon fibre ($\nu \approx 0.25$), we obtain:

$$\sigma_C = \sigma_F \text{ (law of mixtures)} - 2H (1 - V_f) (\nu_m - \nu_f)$$

The effect of this on the nickel matrix composite strength is not significant.
These data also indicate that the strength of the carbon fibres is unaffected
by hydrostatic pressure and this will be assumed for the resin matrix
composite.

If the algebraic sum of the contributions to the composite tensile strength
from the fibres, the resin (which becomes negative at an H of ~ 80 MNm^{-2})
and Poisson's ratio effect is calculated, a linear decrease of the composite

strength with hydrostatic pressure (albeit with a slope < 1) still results:

$$\sigma_C = \sigma_F (1-V_f) \, 0.77H - (1-V_f) \, 0.3H$$

$$= \sigma_F - 0.47H$$

This relationship is reasonably well obeyed for $H > 80$ MNm^{-2} (Fig 17), but it does not in any way account for the pronounced strength maximum, nearly 90% σ_A, at a pressure of ~ 40 MNm^{-2}. This simple approach, though encouraging, is therefore inadequate and mechanisms of transfer of stress at the resin/fibre interface must be considered.

The initial rise of the composite strength with pressure implies that a more efficient mechanism of load transfer from the resin to the fibres becomes possible through the attainment of higher interface stresses. The matrix shear strength thus appears to control the composite strength at atmospheric pressure, as the maximum useful strength of the fibre/matrix interface is the shear strength of the matrix. The initial strengthening, with increasing pressures up to ~ 40 MNm^{-2}, can be interpreted by allowing the interfacial shear stress to rise with pressure with a slope of ~ 0.1. Accordingly, as at $H = 0$,

$$\sigma_C \to \sigma_F = V_f \, \sigma'_f + (1 - V_f) \, \sigma_m$$

$$930 = 0.54 \, \sigma'_f + 0.46 \times 54 \text{ MNm}^{-2},$$

the effective strength of the fibres, σ'_f, is 1670 MNm^{-2}. If it is made to increase with pressure with a slope of 0.11; for $0 < H < 40$ MNm^{-2}:

$$\sigma_C = \sigma_F + 0.54 \times 1670 \times 0.11H/32 - 0.47H$$

$$= \sigma_F + 3.1H - 0.47H = \sigma_F + 2.63H$$

For values of H above ~ 40 MNm^{-2} the resin maximum principal stress becomes compressive and it is seen (Fig 17) that the fall in the composite strength is in accord with a reversal in the "extra" pressure-dependent contribution to the shear stress:

$$\sigma_C = (\sigma_F + 124) - 3.1 (H - 40) - 0.47H = \sigma_F + 104 - 3.6 (H - 40) \text{ MNm}^{-2},$$

until a hydrostatic pressure of 80 MNm^{-2} is applied. Above this pressure the stress system in the resin is wholly compressive, ie the resin is no longer pulled but is being allowed to be squeezed out.

REFERENCES

1. D L McDaniels, R W Jech and J W Weeton, Fiber Reinforced Metallic Composites. Procs of the 6th Sagamore Ordnance Materials Research Conference, August 1959.

2. O Outwater Jr, Modern Plastics, 1956, 33(7), 156, 158, 160, 162.

3. N H Parratt, Defects in glass fibres and their effect on the strength of plastic mouldings, Rubber and Plastics Age, 1960, 41, 263-266.

4. B W Rosen, Tensile failure of fibrous composites, AIAA Journal, 1964, 2, 1985-1991.

5. B W Rosen, Fiber Composite Materials, American Society for Metals Seminar, October 1964.

6. R L McCullough, Concepts of Fiber-Resin Composites, Marcel Dekker, Inc, New York (1971).

7. A Kelly and W R Tyson, in High Strength Materials, Procs of the 2nd Berkeley International Materials Conf, June 1964, pp 578-599 (editor, V F Zackay), Wiley, 1965.

8. A Kelly and G J Davies, The principles of the fibre reinforcement of metals, Metallurgical Reviews, 1965, 10 (37), 1-177.

9. D L McDaniels, R W Jech and J W Weeton, Analysis of stress-strain behavior of tungsten-fiber-reinforced copper composites, Trans Met Soc AIME, 1965, 233 (4), 636-642.

10. J J Dibb, A S Wronski and B Watson-Adams, Composites, 1973, 4 (5), 227-228.

11. G Garnett, N C Hancox and R A P Spencer, Third Conference on Research Projects, Plastics Institute, Nov 1971.

12. B R Watson-Adams, J J Dibb and A S Wronski, Procs of the Liverpool Symposium on Metal Matrix Composites, 1972.

13. C W Kistler and D E Niesz, unpublished United States Report.

14. D M Braddick, P W Jackson and P J Walker, J Materials Sci, 1971, 6 (5), 419-426.

15. P D Donovan and B R Watson-Adams, The formation of composite materials by electrodeposition, Metals and Materials 1969, 3 (11), 443-450.

16. N M Parikh, Fiber Composite Materials, American Soc for Metals Seminar, October 1964.

17.   P W Jackson and J R Marjoram, Compatibility studies of carbon fibres with nickel and cobalt, J Materials Sci, 1970, 5 (1), 9-23.

18.   R B Barclay and W Bonfield, Carbon fibre/nickel compatibility, J Materials Sci, 1971, 6 (0), 1076-1083.

19.   F B Bowden, J Materials Sci, 1970, 5 (6), 517-520.

20.   N H Parratt, Fibre Reinforced Materials Technology (p41), Van Nostrand Reinhold (1972).

21.   A Kelly, private communication.

Reports quoted are not necessarily available to members of the public or to commercial organisations.

$NiSO_4\ 7H_2O$	200g/ℓ
H_3BO_3	30g/ℓ
NaCℓ	20g/ℓ
pH	3·2 TO 3·5

TABLE I WATTS NICKEL BATH : COMPOSITION

TREATMENT	NUMBER OF TESTS	MEAN STRENGTH IN GNm^{-2}	STANDARD DEVIATION IN GNm^{-2}
UNPLATED	23	2·24	0·39
AS PLATED	27	1·56	0·25
24 HRS AT 1050 °C AND ~10^{-6} torr	3	0·092	0·004
24 HRS AT 1050 °C IN SEALED TUBE WITH PURE CARBON POWDER	10	2·41 ± 0·55	0·35

TABLE 2 NICKEL – PLATED FIBRE : STRENGTH DATA

TABLE 3

%Vf	IMPACT STRENGTH $Jm^{-2} \times 10^4$
0	12·7
20	7·9
30	5·1
40	3·1
53	1·9
70	2·9

TABLE 3 THE EFFECT OF Vf ON THE CHARPY IMPACT STRENGTH OF CARBON FIBRE / NICKEL COMPOSITE AT 20 °C

FIG. I

BREAKING STRESS OF FIBRE, σ_f

TENSILE
STRESS
IN FIBRE
σ

$\bar{\sigma}_f$ $\bar{\sigma}_f$ $\bar{\bar{\sigma}}_f$

SHEAR
STRESS
AT INTERFACE
τ

$L < L_c$ $L = L_c$ $L > L_c$

DISCONTINUOUS FIBRE LENGTH, L
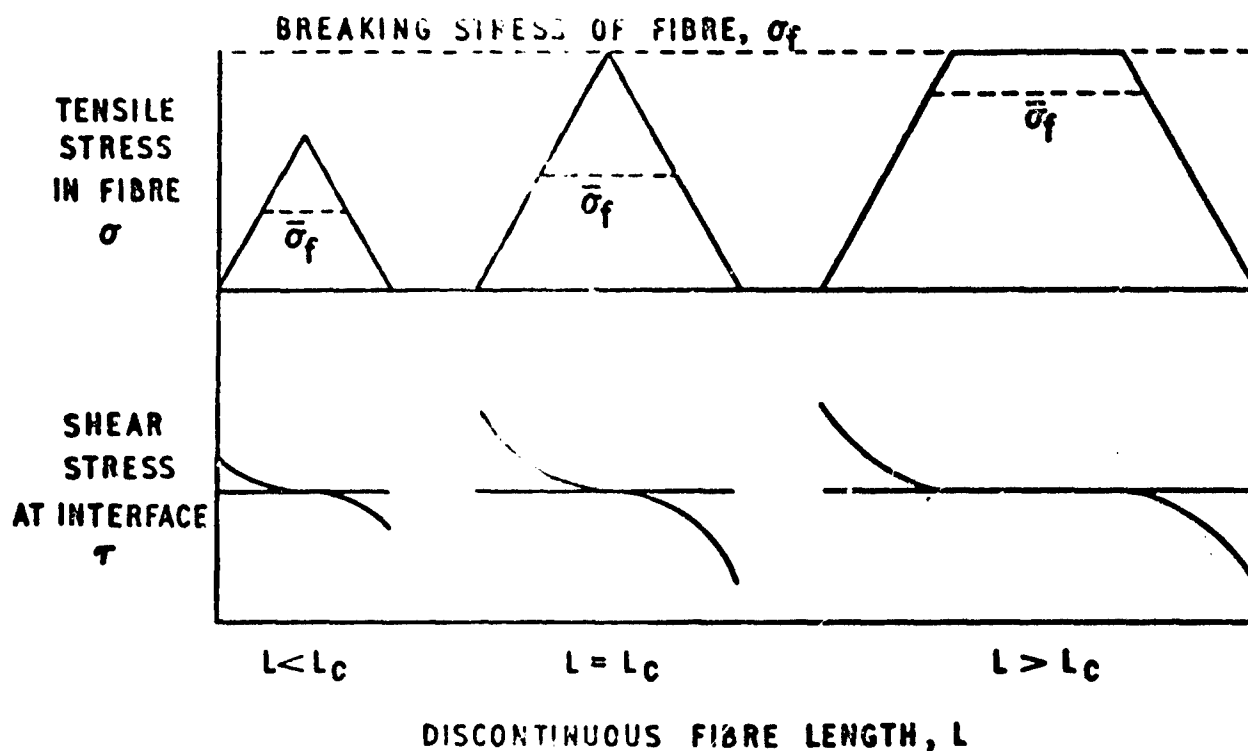
THE VARIATIONS OF THE TENSILE STRESS IN THE FIBRE, σ_f,
AND THE SHEAR STRESS AT THE FIBRE/MATRIX INTERFACE, τ,
WITH DISTANCE FROM THE FIBRE END FOR DISCONTINUOUS FIBRES
OF LENGTH, L; SHORTER THAN, EQUAL TO AND LONGER THAN
THE CRITICAL FIBRE LENGTH, L_c

FIG. I
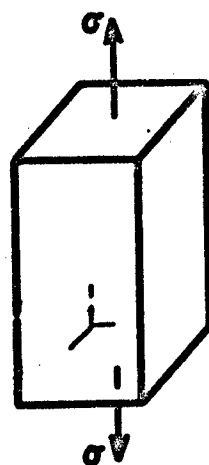
FIG.2

TENSILE STRESS: σ

MAXIMUM SHEAR STRESS: $\frac{1}{2}\,\sigma = \frac{\sigma}{2}$

SIMPLE TENSION
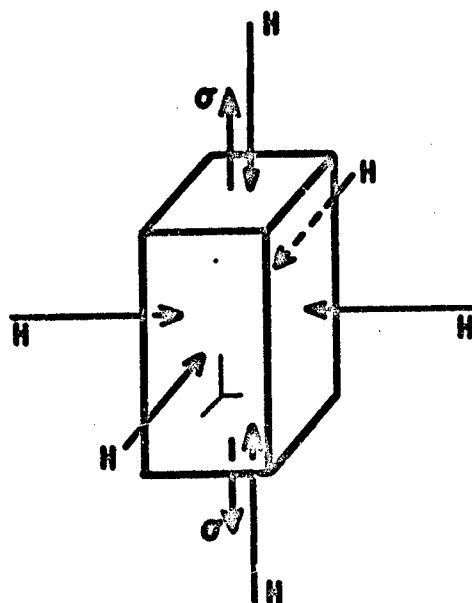
TENSILE STRESS: $\sigma - H$

MAXIMUM SHEAR STRESS:

$$\frac{1}{2}\left\{(\sigma-H)-(-H)\right\} = \frac{\sigma}{2}$$

TENSION under superposed HYDROSTATIC PRESSURE

FIG.2 MAXIMUM SHEAR STRESS IN A SIMPLE TENSION TEST AT
ATMOSPHERIC AND UNDER SUPERPOSED HYDROSTATIC PRESSURE, H

FIG. 3

STEEL CABLE

PULTRUDED ROD

DIE SURROUNDED BY HEATING COILS

WATER COOLED DIE ENTRANCE

WATER

TENSIONING ROLLER

RESIN CONTROL ORIFICES

RESIN BATH

CARBON FIBRE TOWS

ELECTRIC MOTOR AND CABLE DRUM

RESIN IMPREGNATED CARBON FIBRE TOWS

SCISSORS LIFT
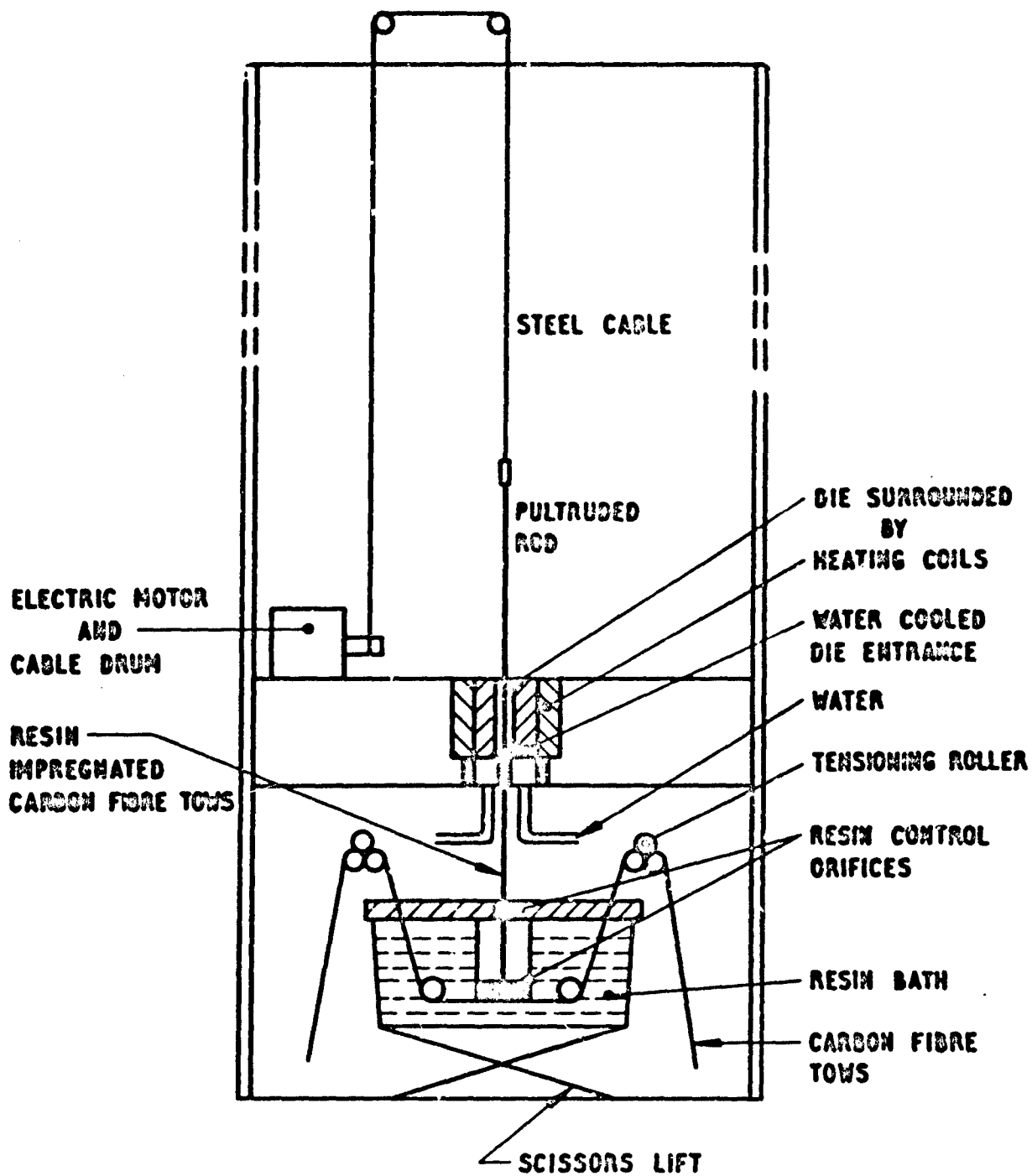
FIG. 3 PULTRUSION APPARATUS (SCHEMATIC)
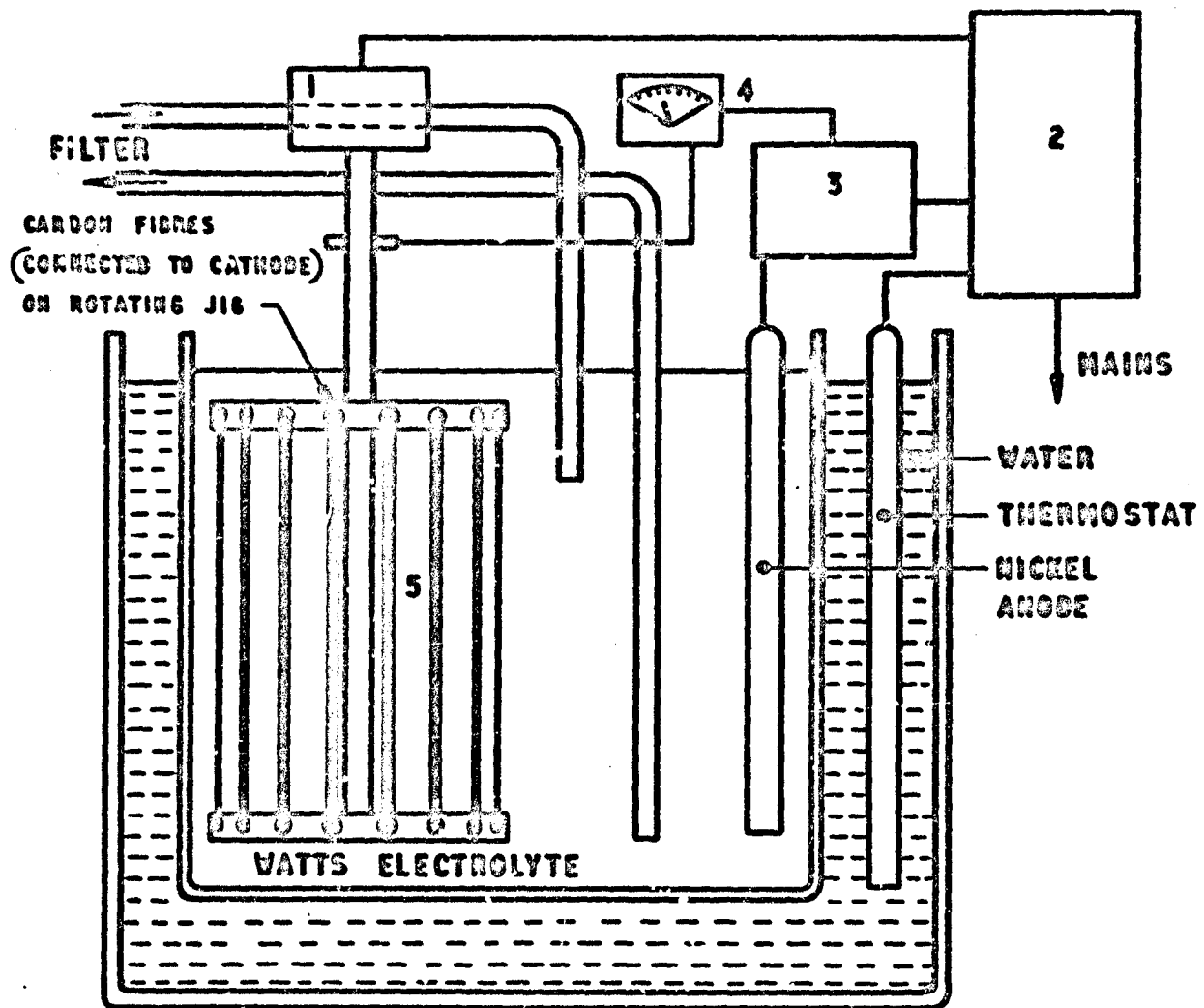
FIG.4 NICKEL PLATING BATH
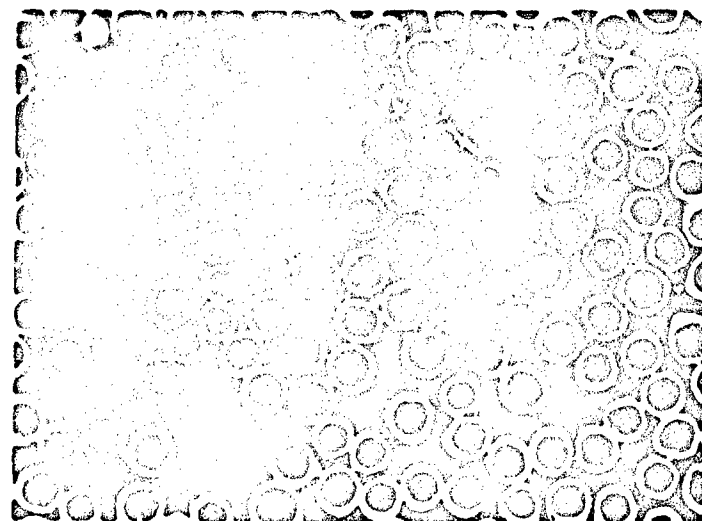
FIG.5 CROSS SECTION OF AS-PLATED FIBRES

FIG 6
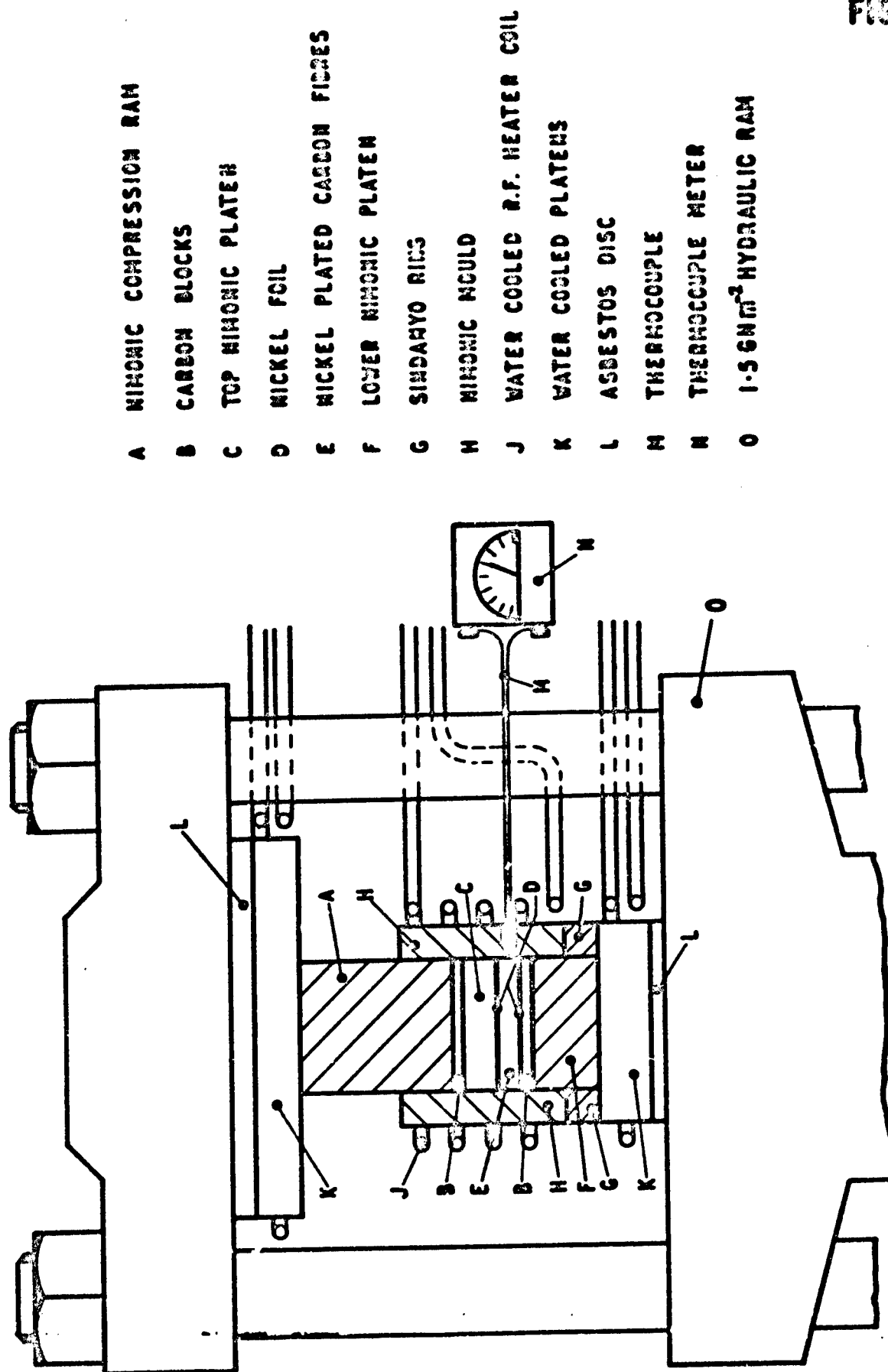
A NIMONIC COMPRESSION RAM

B CARBON BLOCKS

C TOP NIMONIC PLATEN

D NICKEL FOIL

E NICKEL PLATED CARBON FIBRES

F LOWER NIMONIC PLATEN

G SINDANYO RING

H NIMONIC MOULD

J WATER COOLED R.F. HEATER COIL

K WATER COOLED PLATENS

L ASBESTOS DISC

M THERMOCOUPLE

N THERMOCOUPLE METER

O 1·5 GNm⁻² HYDRAULIC RAM

FIG.6 ASSEMBLY FOR COMPACTING PLATED CARBON FIBRES
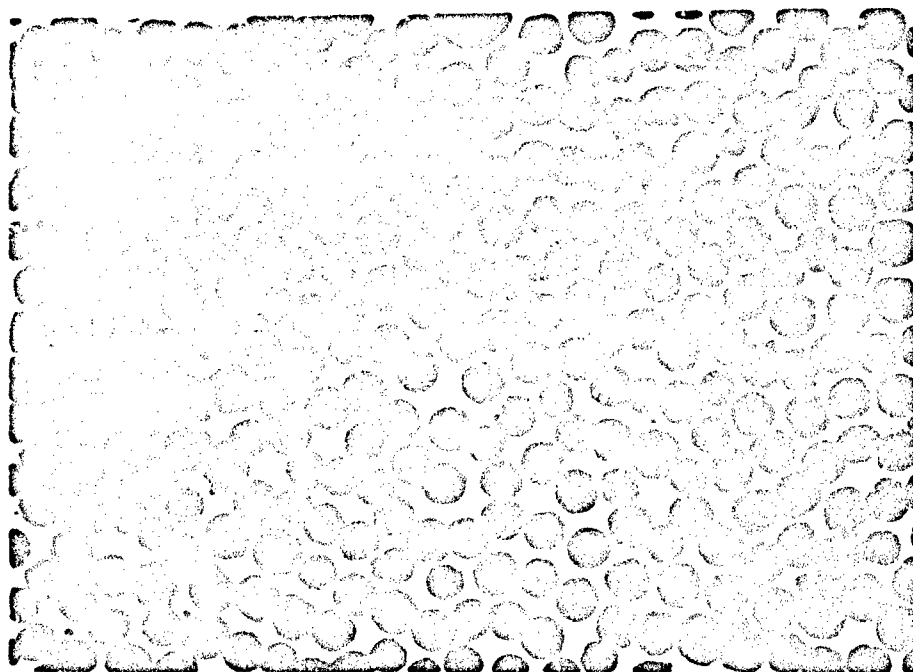
X 600

FIG. 7   CROSS-SECTION OF CARBON FIBRE/NICKEL COMPOSITE
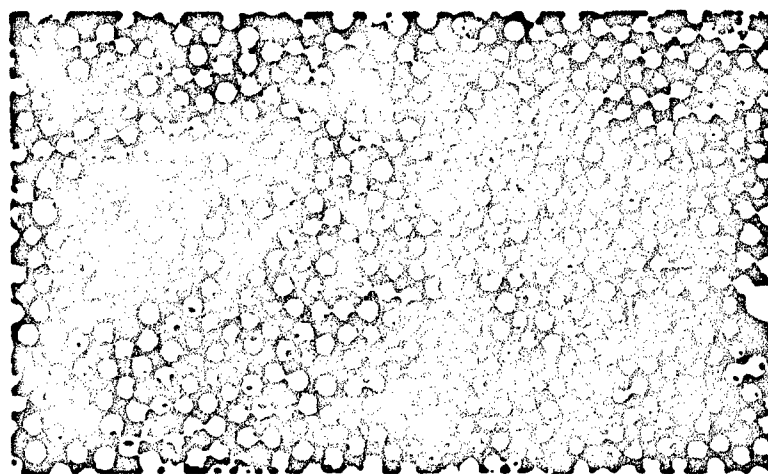
100 μm

FIG. 8   CROSS-SECTION OF CARBON FIBRE/EPOXY RESIN COMPOSITE

FIG. 9
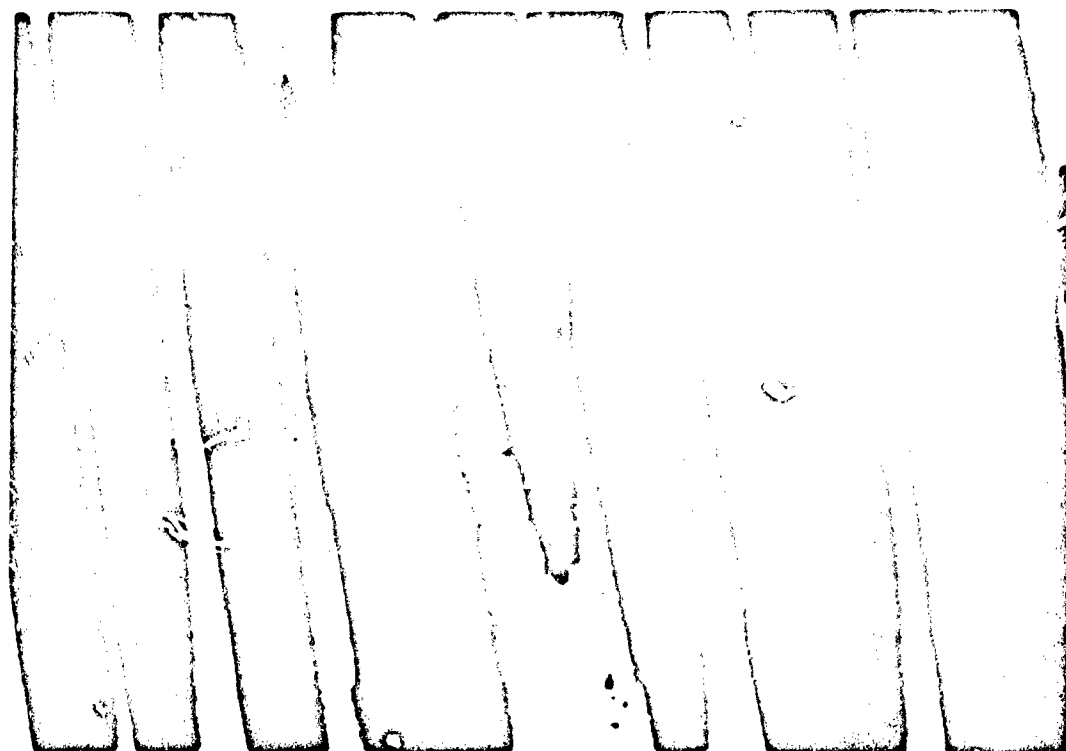
X 1000

FIG. 9 LONGITUDINAL SECTION OF CARBON FIBRE/NICKEL COMPOSITE
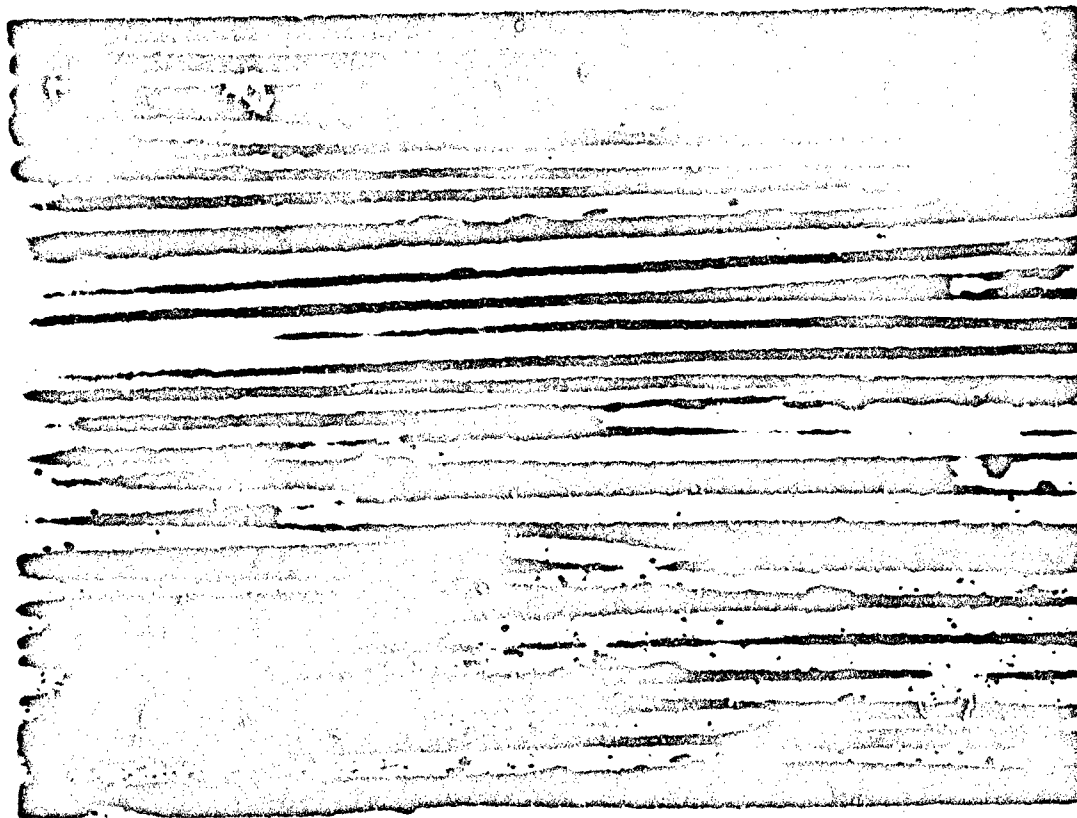
FIG.10 LONGITUDINAL SECTION OF CARBON FIBRE / EPOXY RESIN COMPOSITE
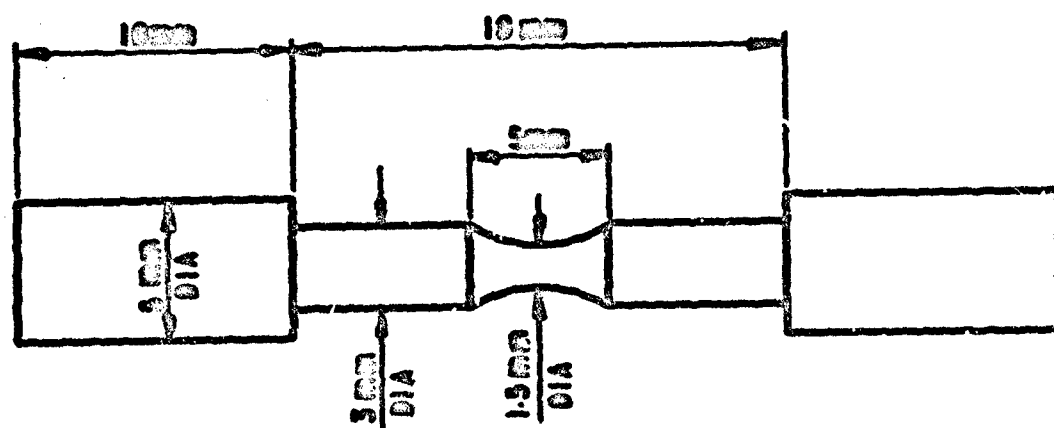
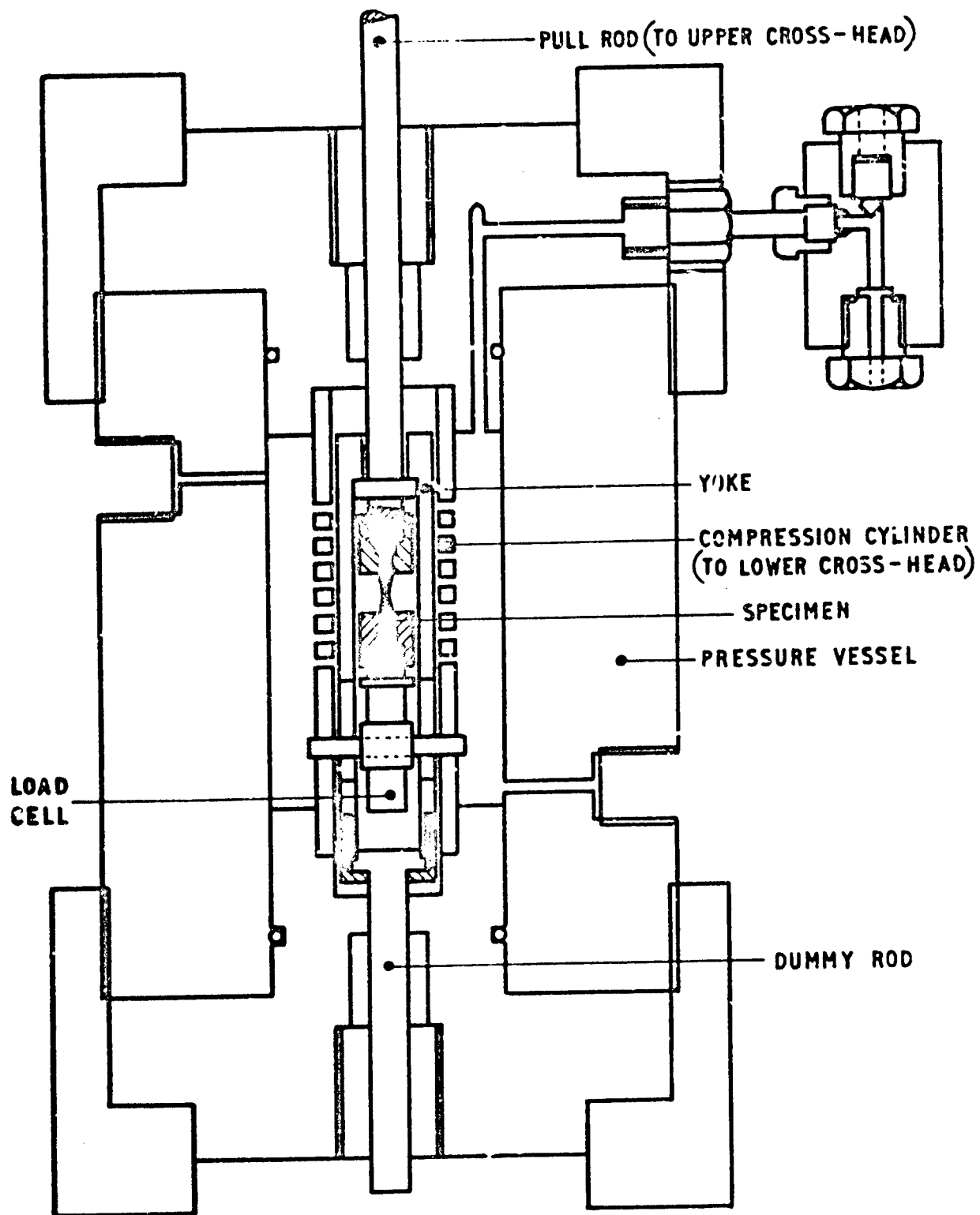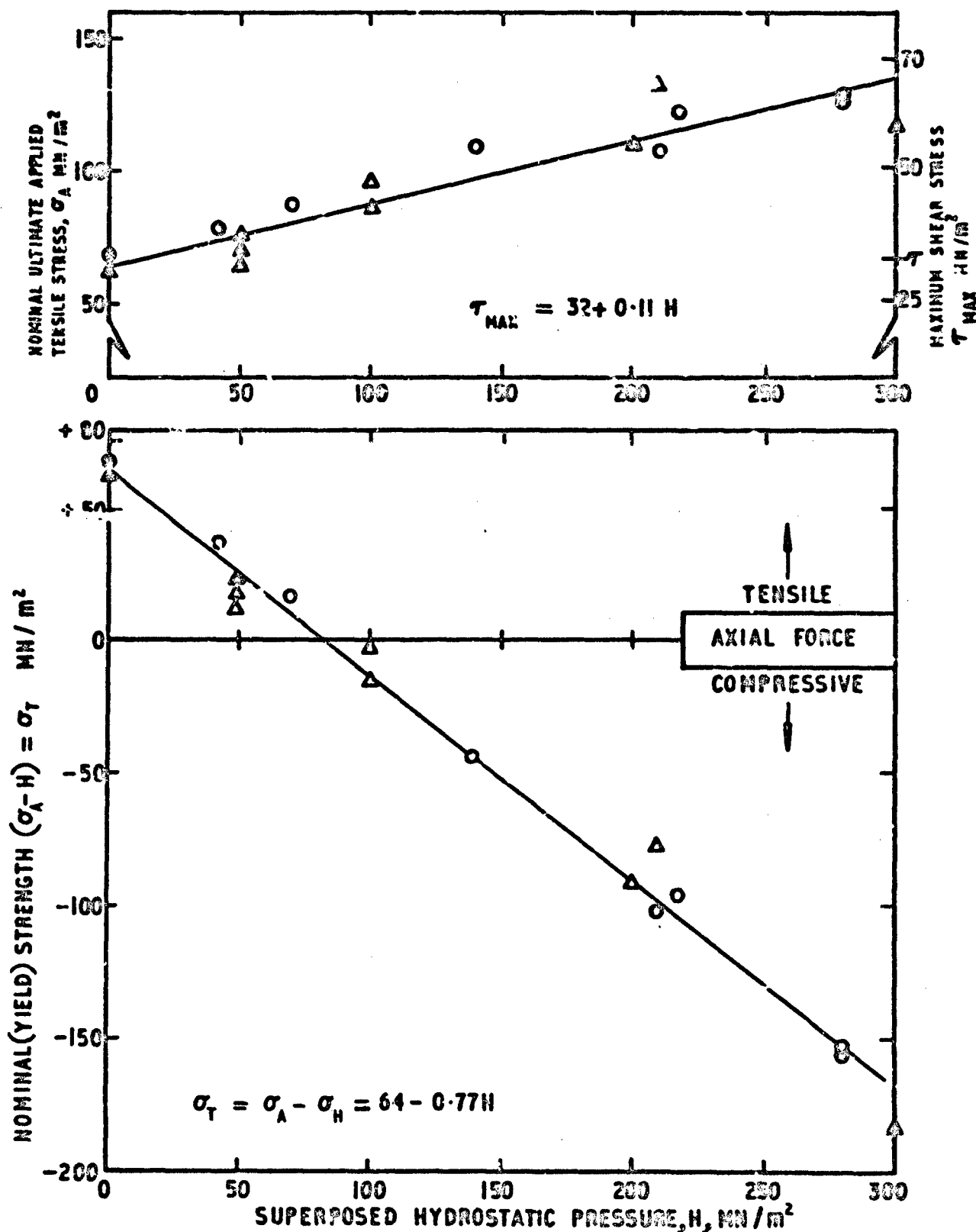FIG.11 EPOXY TENSILE SPECIMEN DESIGN

FIG. 12

PULL ROD (TO UPPER CROSS-HEAD)

YOKE

COMPRESSION CYLINDER
(TO LOWER CROSS-HEAD)

SPECIMEN

PRESSURE VESSEL

LOAD
CELL

DUMMY ROD

FIG. 12 THE ASSEMBLY FOR TENSILE TESTING UNDER
SUPERPOSED HYDROSTATIC PRESSURE

FIG.13

$$\tau_{MAX} = 32 + 0.11 H$$

$$\sigma_T = \sigma_A - \sigma_H = 64 - 0.77 H$$

TENSILE

AXIAL FORCE

COMPRESSIVE

O △ - THE TWO SYMBOLS REFER TO TWO DIFFERENT BATCHES OF SPECIMENS

FIG.13 THE EFFECT OF HYDROSTATIC PRESSURE ON THE TENSILE
AND SHEAR STRENGTH OF PLASTICISED EPOXY RESIN

FIG.14
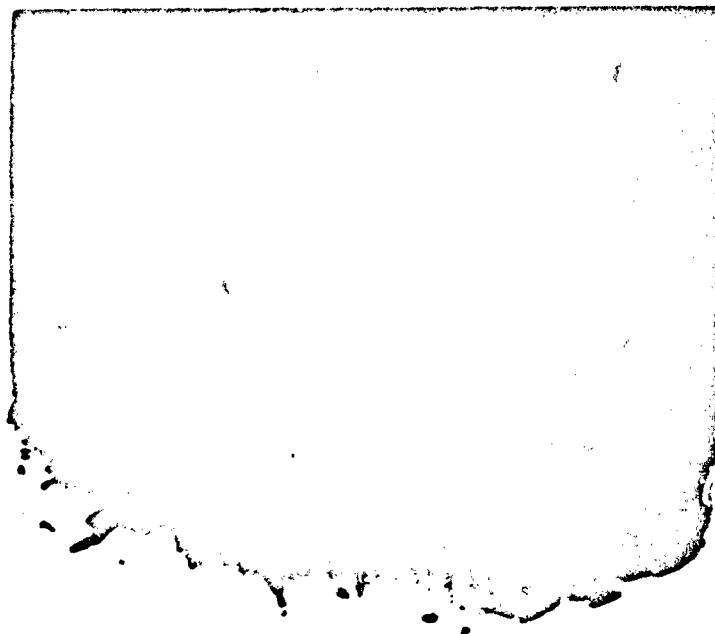
200 μm

FIG. 14   SCANNING ELECTRON MICROGRAPH OF THE FAILURE FACE OF A PLASTICIZED
         EPOXY RESIN SPECIMEN FRACTURED AT ATMOSPHERIC PRESSURE.

FIG. 15

50 μm

FIG. 15 SCANNING ELECTRON MICROGRAPH OF THE FAILURE FACE OF
A PLASTICIZED EPOXY RESIN SPECIMEN TESTED IN TENSION
UNDER SUPERPOSED HYDROSTATIC PRESSURE OF 300 MN/m^2.
THE APPLIED TENSILE LOAD WAS 125 MN/m^2, IE THE AXIAL
STRESSES COMPRESSIVE. NOTE THE SHEAR LIP (CENTRAL
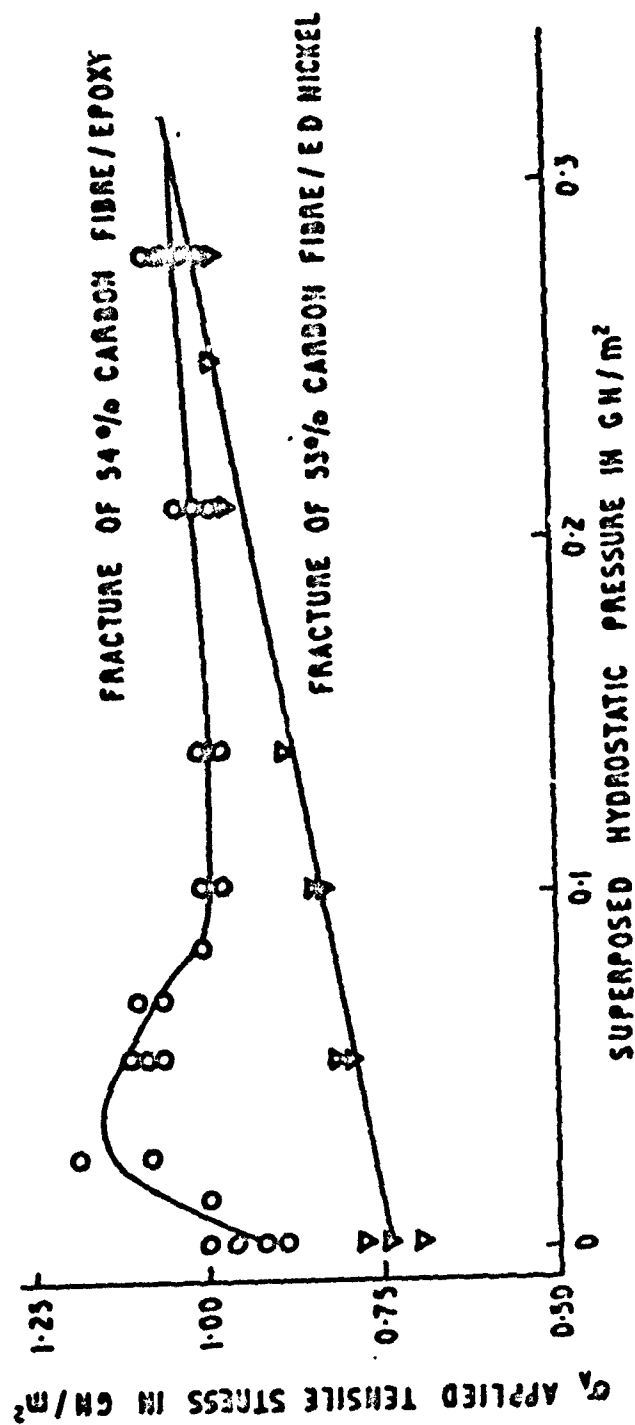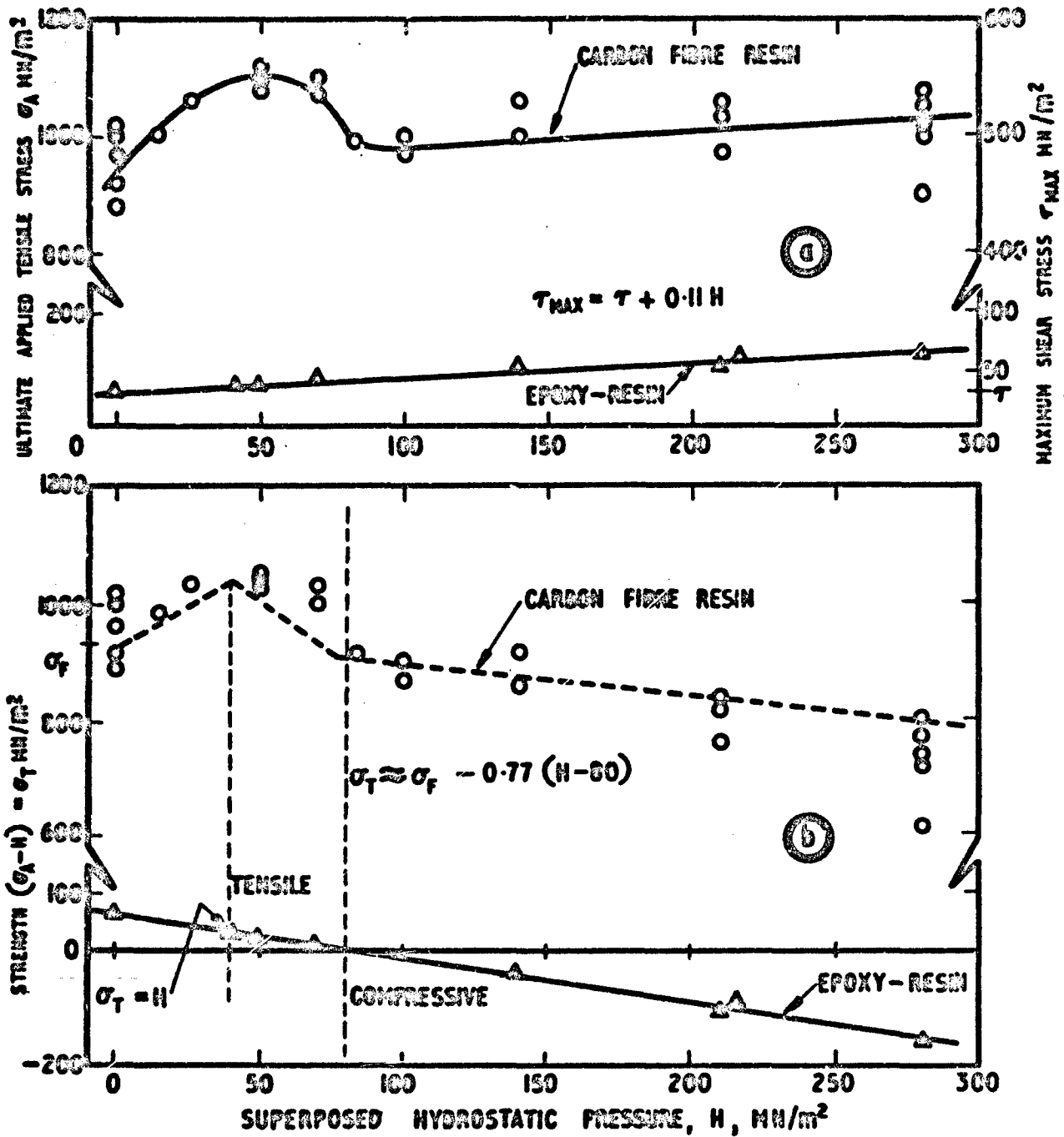FAILURE COULD HAVE BEEN CAUSED AS A RESULT OF FLUID
PENETRATION).

FIG. 16

FIG.16 THE INFLUENCE OF HYDROSTATIC PRESSURE ON THE FRACTURE STRENGTH

(a) THE EFFECT OF HYDROSTATIC PRESSURE ON THE TENSILE STRENGTH OF THE CARBON FIBRE/RESIN COMPOSITE AND THE TENSILE AND SHEAR STRENGTHS OF THE RESIN.

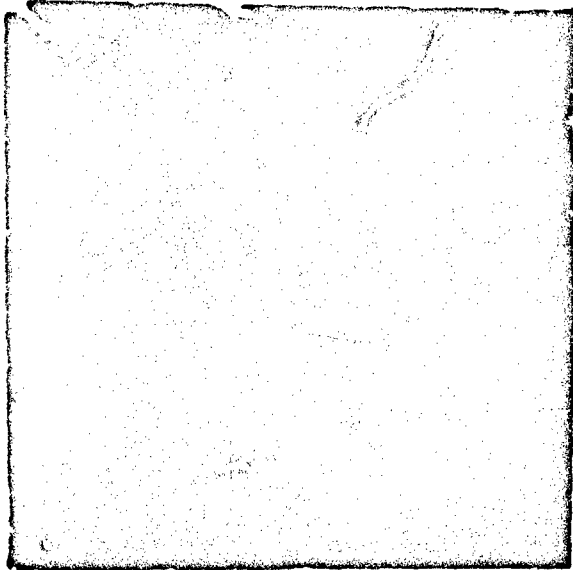(b) THE DASHED PLOTS REPRESENT THE CALCULATED COMPOSITE STRENGTH.

FIGS. I7(a)(b)

FIG. 18 CARBON FIBRE/EPOXY RESIN COMPOSITE FAILURE SURFACE
TESTED AT ATMOSPHERIC PRESSURE

FIG. 19 AS FIG. 18, TESTED UNDER A SUPERIMPOSED HYDROSTATIC
PRESSURE OF 200 Nm^{-2}

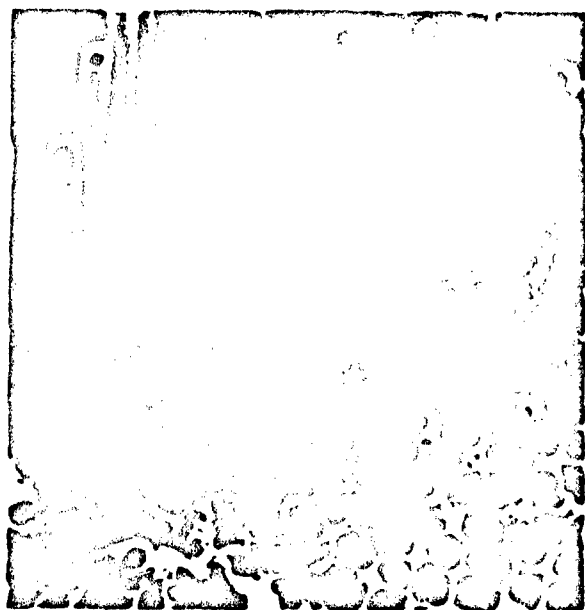(a) CARBON FIBRE REINFORCED NICKEL FAILURE SURFACE. ATMOSPHERIC PRESSURE.

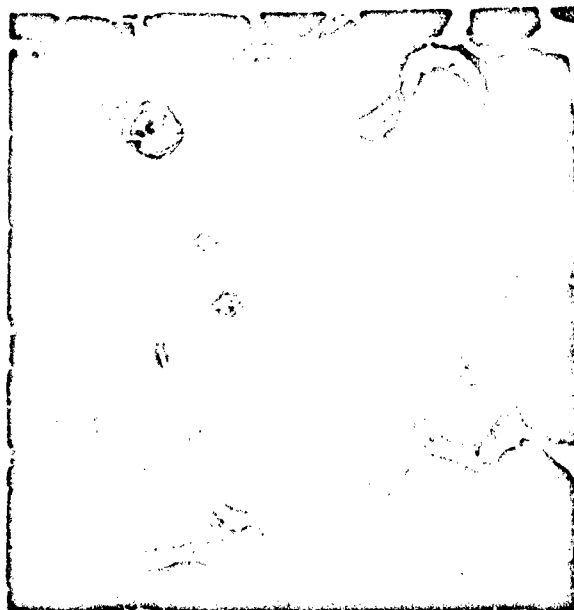(b) AS (a) TESTED AT A SUPERPOSED HYDROSTATIC PRESSURE OF 100 MNm^{-2}

(c) AS (a) TESTED AT A SUPERPOSED HYDROSTATIC PRESSURE OF 200 MNm^{-2}
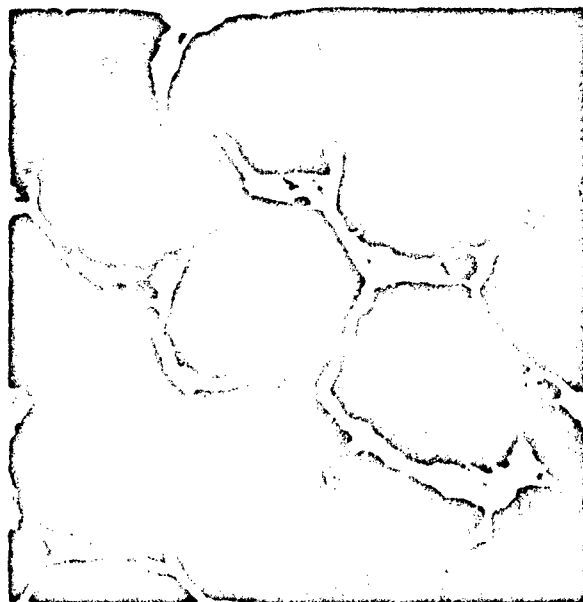
FIGS. 20(a)(b)(c)

(a) 'TRANSITION' REGION FROM
    TENSILE TO COMPRESSIVE FAILURE
    OF FIBRES AT 500°C

(b) 'COMPRESSIVE' FAILURE AT ROOM
    TEMPERATURE. NOTE THE SIMILARITY
    OF THE NICKEL FAILURE MODE TO
    THAT IN SIMPLE TENSION, FIG. 20(a)

(c) SAME AS (a) DETAIL OF 'COMPRESSIVE' FAILURE.
    NOTE THE DUCTILE FAILURE OF THE MATRIX

FIG. 21   SCANNING ELECTRON MICROGRAPHS OF THE FAILURE SURFACES OF
         MINIATURE CHARPY IMPACT SPECIMENS OF THE CARBON FIBRE/NICKEL COMPOSITE

DOCUMENT CONTROL SHEET

(Notes on completion overleaf)

Overall security classification of sheet ......[UNCLASSIFIED]..

(As far as possible this sheet should contain only unclassified information. If is is necessary to enter classified information, the box concerned must be marked to indicate the classification eg (R),(C) or (S)).

1. DRIC Reference (if known)	2. Originator's Reference RARDE TECH REPORT 19/75	3. Agency Reference	4. Report Security Classification UNLIMITED
5. Originator's Code (if known) 851600	6. Originator (Corporate Author) Name and Location ROYAL ARMAMENT R&D EST MINISTRY OF DEFENCE UK		
5a. Sponsoring Agency's Code (if known)	6a. Sponsoring Agency (Contract Authority) Name and Location		

7. Title	Mechanical properties of fibre-reinforced composites tested under superposed hydrostatic pressures.

7a. Title in Foreign Language (in the case of translations)

7b. Presented at (for conference papers). Title, place and date of conference

8. Author 1.Surname, initials WATSON-ADAMS B R	9a Author 2 DIEB J J	9b Authors 3, 4... WRONSKI A S	10. Date 11 1975	pp 32	ref 21
11. Contract Number K2/2168/012/RAR/B	12. Period	13. Project	14. Other References		

15. Distribution statement

No limitations _

Descriptors (or keywords)

Fibre composites. Tensile strength. Impact strength. Hydrostatic pressure.

(TEST)

continue on separate piece of paper if necessary

Abstract

The tensile strengths of glass fibre or carbon fibre/resin composites are generally in the order of 60% of the theoretically predicted values. 50% carbon fibre and 60% glass fibre/epoxy resin composite rods were produced by pultrusion and these gave tensile strengths of about 80% theoretical. This result suggests than an "effective discontinuous fibre length" is an important composite parameter. Tensile testing of these composites under superposed hydrostatic pressure has increased the value to 90% theoretical.

50% carbon fibre/nickel composites produced by a plating and hot compaction